Hypoxia induces severe right ventricular dilatation and infarction in heme oxygenase-1 null mice

Rapid PUBLICATION

Shaw-Fang Yet,[1] Mark A. Perrella,[1,2,3] Matthew D. Layne,[1] Chung-Ming Hsieh,[1] Koji Maemura,[1] Lester Kobzik,[4] Philippe Wiesel,[1] Helen Christou,[5] Stella Kourembanas,[5] and Mu-En Lee[1,2,6]

[1]Cardiovascular Biology Laboratory, Harvard School of Public Health, Boston, Massachusetts 02115, USA
[2]Department of Medicine, Harvard Medical School, Boston, Massachusetts 02115, USA
[3]Pulmonary and Critical Care Division, Brigham and Women's Hospital, Boston, Massachusetts 02115, USA
[4]Department of Environmental Health, Harvard School of Public Health, and Department of Pathology, Harvard Medical School, Boston, Massachusetts 02115, USA
[5]Division of Newborn Medicine, The Children's Hospital, and Department of Pediatrics, Harvard Medical School, Boston, Massachusetts 02115, USA
[6]Cardiovascular Division, Brigham and Women's Hospital, Boston, Massachusetts 02115, USA

Address correspondence to: Mu-En Lee, Cardiovascular Biology Laboratory, Harvard School of Public Health, 677 Huntington Avenue, Boston, Massachusetts 02115, USA. Phone: (617) 432-4994; Fax: (617) 432-0031; E-mail: lee@cvlab.harvard.edu

Received for publication December 30, 1998, and accepted in revised form February 25, 1999.

Heme oxygenase (HO) catalyzes the oxidation of heme to generate carbon monoxide (CO) and bilirubin. CO increases cellular levels of cGMP, which regulates vascular tone and smooth muscle development. Bilirubin is a potent antioxidant. Hypoxia increases expression of the inducible HO isoform (HO-1) but not the constitutive isoform (HO-2). To determine whether HO-1 affects cellular adaptation to chronic hypoxia in vivo, we generated HO-1 null (HO-1$^{-/-}$) mice and subjected them to hypoxia (10% oxygen) for five to seven weeks. Hypoxia caused similar increases in right ventricular systolic pressure in wild-type and HO-1$^{-/-}$ mice. Although ventricular weight increased in wild-type mice, the increase was greater in HO-1$^{-/-}$ mice. Similarly, the right ventricles were more dilated in HO-1$^{-/-}$ mice. After seven weeks of hypoxia, only HO-1$^{-/-}$ mice developed right ventricular infarcts with organized mural thrombi. No left ventricular infarcts were observed. Lipid peroxidation and oxidative damage occurred in right ventricular cardiomyocytes in HO-1$^{-/-}$, but not wild-type, mice. We also detected apoptotic cardiomyocytes surrounding areas of infarcted myocardium by terminal deoxynucleotide transferase–mediated dUTP nick end-labeling (TUNEL) assays. Our data suggest that in the absence of HO-1, cardiomyocytes have a maladaptive response to hypoxia and subsequent pulmonary hypertension.

J.Clin. Invest. **103:**R23–R29 (1999).

Introduction

Heme oxygenase (HO) catalyzes the oxidation of heme to carbon monoxide (CO) and biliverdin, which is reduced subsequently to bilirubin (1). CO, like nitric oxide, is a gas molecule that stimulates guanylyl cyclase and increases intracellular levels of cGMP (1, 2). cGMP is an important regulator of vascular tone and smooth muscle development (3, 4). By degrading the pro-oxidant heme and generating the antioxidant bilirubin (5, 6), HO may also protect cells against oxidative injury (1). Three HO isoforms have been identified. HO-1, also known as heat shock protein 32 (7, 8), is a 32-kDa protein induced by heat, heme, heavy metals, hypoxia, hyperoxia, shear stress, stretch, ultraviolet light, cytokines, and reactive oxygen species (1, 9). HO-2 is a constitutive, 36-kDa isoform (10, 11). HO-3, whose sequence is highly homologous to that of HO-2, has been cloned recently but has not been characterized fully (12).

Under normal physiological conditions, HO-1 and HO-2 are both expressed at low levels in vascular smooth muscle cells (VSMCs) and cardiomyocytes (13–15). Under pathophysiological conditions, however, HO-1, but not HO-2, is induced in the heart and blood vessels (13–17). For example, we and others have reported that bacterial endotoxin markedly increases HO-1 expression in VSMCs and cardiomyocytes in vivo (15, 17, 18). HO-1 is upregulated at both the mRNA and the protein levels in cultured VSMCs exposed to stretching and shear stress (19).

Hypoxia causes a remodeling of the pulmonary vasculature that is characterized by proliferation of VSMCs and deposition of matrix. Hypoxia also increases pulmonary vascular resistance (leading to pulmonary hypertension) and induces right ventricular hypertrophy in humans, rats, and mice (20–24). CO released by HO-1 has been implicated in the regulation of VSMC proliferation and may regulate vascular remodeling in response to hypoxia (13, 25). In addition, pressure overload of the right ventricle, induced experimentally by hypoxia or pulmonary artery banding, increases HO-1 expression in rat cardiomyocytes (26). Taken together, these data suggest an important role for HO-1 in cardiovascular adaptation to hypoxic stress.

To gain insight into the biologic functions of HO-1 in vivo, we generated HO-1 null (HO-1$^{-/-}$) mice by targeted mutation. We subjected the mice to chronic hypoxia, which induces pulmonary hypertension, to study the function of HO-1 in the cardiovascular system.

Methods

Targeted disruption of HO-1 in embryonic stem cells and generation of HO-1$^{-/-}$ mice. To make the HO-1 targeting construct, we isolated genomic clones from a 129 SvJ mouse λDASH II genomic library (Stratagene, La Jolla, California, USA). Subcloning was per-

formed according to the published HO-1 restriction map (27). The plasmid pHO-neo was constructed by inserting the *Xho*I-*Bam*HI neomycin resistance gene (*neo*) expression cassette from pMC1neo polyA (Stratagene) into pBluescript II SK (Stratagene), followed by an *Xho*I HO-1 genomic fragment containing 3 kb of 5′ upstream sequence at the *Xho*I site. A *Bam*HI-*Eco*RI HO-1 fragment containing 3 kb of 3′ downstream sequence was inserted into thymidine kinase gene (*TK*) plasmid pPGK-TK. A 6-kb *Cla*I (filled in)-*Bam*HI fragment containing a TK expression cassette and the 3′ arm of the HO-1 genomic sequence was subsequently subcloned into the *Xba*I (filled in)-*Bam*HI site of pHO-neo to generate the HO-1 targeting construct.

The HO-1 targeting construct was linearized with *Not*I before electroporation into D3 embryonic stem (ES) cells. Clones were selected in growth medium containing G418 and ganciclovir (28), and correctly targeted ES clones were identified by Southern blot analysis. These targeted ES cells were injected into BALB/c and C57BL/6 blastocysts to generate chimeric mice (Core Transgenic Mouse Facility, Brigham and Women's Hospital). Male chimeras were mated to BALB/c and C57BL/6 females, and heterozygous offspring were intercrossed to generate HO-1$^{-/-}$ mice. Mice used for the experiments were maintained on a 129 Sv × BALB/c mixed genetic background. All animal experiments were performed in accordance with National Institutes of Health guidelines, and all protocols were approved by the Harvard Medical Area Standing Committee on Animals.

Southern and Northern blot analysis. Genomic DNA was prepared from ES cells or mouse-tail biopsies (29), digested with *Bam*HI, fractionated on 0.8% agarose gels, and transferred to nylon membranes. The membranes were then hybridized with a random-primed, ^{32}P-labeled 5′ external probe (*Eco*RI-*Xho*I fragment, 5′ probe bar; Figure 1a). Total liver RNA was isolated from embryonic day (E) 18.5 mice by using RNAzol B according to the manufacturer's instructions (Tel-Test Inc., Friendswood, Texas, USA). RNA was fractionated on 1.3% agarose (6% formaldehyde) gels and transferred to nitrocellulose filters. The filters were hybridized with random-primed, ^{32}P-labeled HO-1 or HO-2 cDNA probes (13) as described (15). Equal loading was verified by hybridizing the filters to a ^{32}P-labeled oligonucleotide complementary to 18S ribosomal RNA.

Western blot analysis. Total protein was prepared by homogenizing E18.5 liver in 25 mM Tris (pH 7.5), 50 mM NaCl, and 10 mM EDTA containing Complete protease inhibitors (Boehringer Mannheim Biochemicals, Indianapolis, Indiana, USA). Aliquots containing 25 μg of protein were fractionated on 10% tricine-SDS-polyacrylamide gels and then transferred to nitrocellulose filters. The filters were incubated with a polyclonal anti–HO-1 antiserum (SPA-895; StressGen Biotechnologies Corp., Victoria, British Columbia, Canada) diluted 1:1,000 or with a polyclonal anti–HO-2 antiserum (OSA-200; StressGen Biotechnologies Corp.) diluted 1:2,000, and then incubated with horseradish peroxidase–conjugated goat anti-rabbit serum. Membranes were processed with an enhanced chemiluminescence reagent (Pierce Chemical Co., Rockford, Illinois, USA) and exposed to film.

Hypoxic exposure. Wild-type and HO-1$^{-/-}$ littermates (11–12 weeks old) were exposed to normobaric hypoxia (a 10% oxygen environment) for five to seven weeks as described (30). Age-matched control mice were maintained in ambient oxygen. Five to six animals were studied in each group in each experiment.

Hemodynamic measurements. Mice were anesthetized with chloral hydrate (0.54 mg/g body weight). The trachea was cannulated with a tubing adapter, and the mouse was placed on a ventilator (fractional inspired oxygen concentration 21%; tidal volume 0.01 ml/g). The thoracic cavity was then opened, and PE-50 polyethylene tubing (Clay Adams, Parsippany, New Jersey, USA)

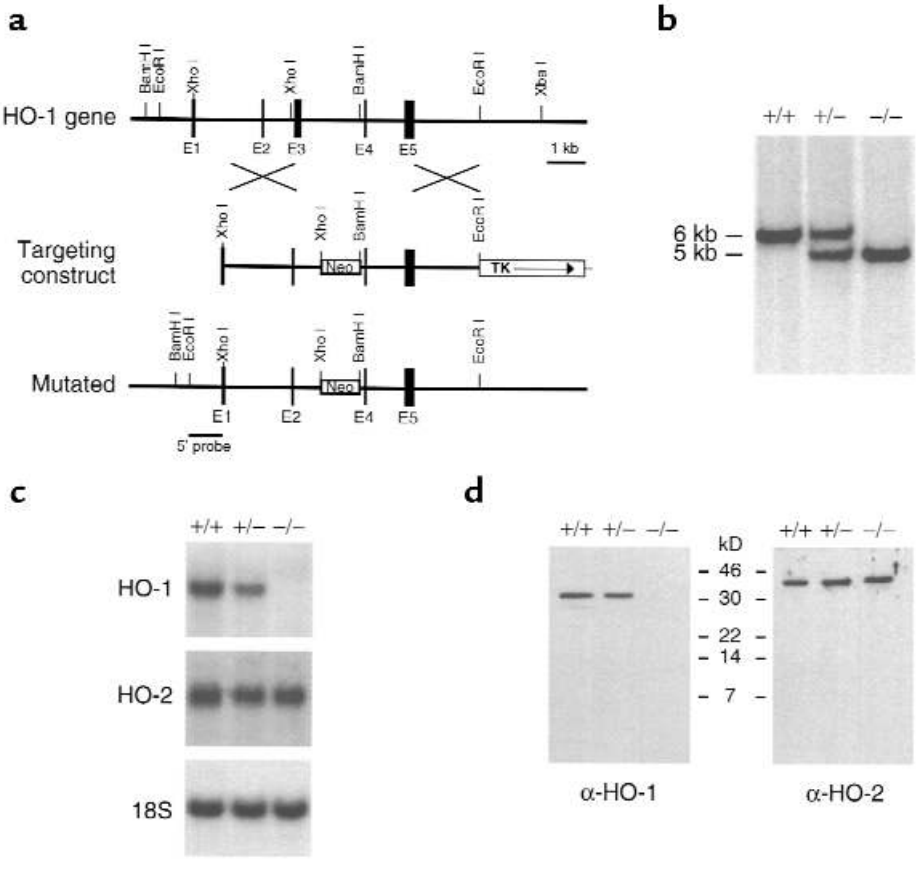

Figure 1
Targeted disruption of the mouse HO-1 gene. (**a**) Diagram of the mouse HO-1 locus (top), the targeting construct (middle), and the predicted mutated allele (bottom). The position of the 5′ probe, external to the targeting construct and internal to the *Bam*HI sites used to characterize the targeted locus, is shown at the bottom. (**b**) Southern blot analysis of *Bam*HI–digested genomic DNA from offspring of HO-1 heterozygote matings. The 5′ probe was hybridized to a 6-kb endogenous fragment and a 5-kb mutated fragment. (**c**) Northern blot analysis of liver RNA from E18.5 mice that were wild-type (+/+), heterozygous (+/−), or homozygous (−/−) for the targeted HO-1 allele. The blots were probed sequentially for expression of HO-1, HO-2, and 18S (to verify equivalent loading). (**d**) Total liver protein was extracted from E18.5 mice. Aliquots (25 μg) were subjected to Western blotting with a polyclonal anti–HO-1 antiserum (α-HO-1, left) or a polyclonal anti–HO-2 antiserum (α-HO-2, right).

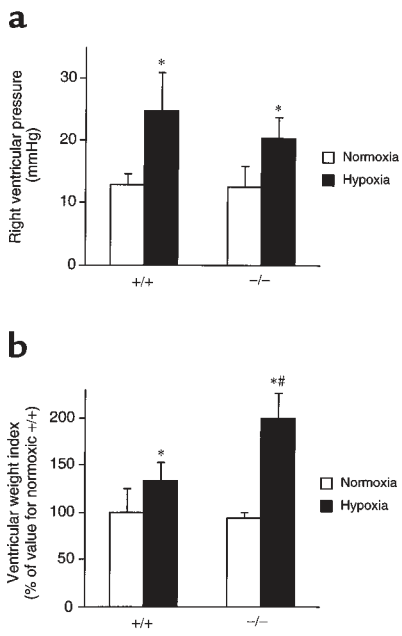

Figure 2
Chronic hypoxia increases right ventricular systolic pressure and ventricular weight in wild-type and HO-1$^{-/-}$ mice. Wild-type (+/+) and HO-1 null (–/–) mice were exposed to normoxia or chronic hypoxia (10% oxygen). (**a**) Right ventricular systolic pressure was measured under normoxic conditions (open bars) or after five weeks of hypoxia (filled bars). Error bars indicate standard deviations. *P < 0.05 vs. animals exposed to normoxia within the same group (n = 5 in each group). (**b**) Ventricular weight in wild-type and HO-1$^{-/-}$ mice was measured under normoxic conditions (n = 6 in each group) or after seven weeks of hypoxia (n = 5 in each group) and expressed as a ratio of ventricular weight (milligrams) to total body weight (grams). The value obtained for normoxic wild-type mice (4.46 ± 0.52) was set as 100%. The ventricular weight index for mice housed under normoxic (open bars) or hypoxic (filled bars) conditions is expressed relative to the value for normoxic wild-type mice. Error bars indicate standard deviations. *P < 0.05 vs. animals exposed to normoxia within the same group. #P < 0.05 vs. wild-type animals exposed to hypoxia.

was inserted into the right ventricle. Right ventricular systolic pressure was measured with MacLab monitoring equipment from CB Sciences (Dover, New Hampshire, USA) as described (15).

Ventricular weight measurements. Hearts were excised, atria were removed, and ventricles were blotted and weighed. Ventricular weight was normalized to total body weight (grams).

Histological analysis, immunocytochemistry, and TUNEL assay. Ventricles were fixed in 4% paraformaldehyde overnight at 4°C and embedded in paraffin. Sections were stained with hematoxylin and eosin or Masson's trichrome. To detect oxidation-specific lipid-protein adducts, we immunostained heart sections with polyclonal antibody MAL-2 (anti–malondialdehyde-lysine; generously provided by J. Witztum, Immunology Core of the La Jolla SCOR Program in Molecular Medicine and Atherosclerosis, La Jolla, California, USA) as described (31) and counterstained them with methyl green. Terminal deoxynucleotide transferase–mediated dUTP nick end-labeling (TUNEL) was used to detect DNA breaks in apoptotic cells in situ (32). Red staining in the nuclei indicated a positive reaction. These tissues were also counterstained with methyl green. Pulmonary vascular remodeling was assessed in lungs that had been perfused with saline through the pulmonary artery and fixed with 4% paraformaldehyde instilled through the trachea (30). Muscularization of peripheral vessels was determined as described (24).

Results

Generation of HO-1$^{-/-}$ mice. To generate a null mutation at the HO-1 locus, we constructed a targeting vector in which HO-1 exon 3 had been replaced with the neomycin resistance gene (*neo*). The thymidine kinase gene (*TK*) was included as a negative selection marker to prevent nonhomologous recombination (Figure 1a). ES cells heterozygous for the targeted HO-1 allele were used to generate chimeric mice. The breeding of chimeras with wild types resulted in transmission of the mutation through the germline. Heterozygotes were intercrossed to generate HO-1$^{-/-}$ homozygotes, as determined by Southern blot analysis (Figure 1b). To confirm the null mutation, we performed Northern blot analysis on RNA isolated at E18.5. HO-1 mRNA levels were lower in heterozygotes than in wild-type mice, and HO-1 mRNA was undetectable in HO-1$^{-/-}$ mice (Figure 1c). HO-2 mRNA levels, in contrast, did not differ significantly among the three genotypes (Figure 1c). We confirmed the null mutation further by Western blot analysis for HO-1 protein. Consistent with the Northern blot analysis, HO-1 protein was not detectable in HO-1$^{-/-}$ mice (Figure 1d). The level of HO-2 protein did not change in HO-1$^{-/-}$ mice (Figure 1d).

Genotyping of three-week-old mice from HO-1 heterozygote matings revealed that the survival rate of HO-1$^{-/-}$ mice was ~7%, consistent with the observations of Poss and Tonegawa (33) about their line of HO-1$^{-/-}$ mice, described while our work was in progress. Among the newborn mice from heterozygote breedings, ~20% were homozygous mutants, indicating partial embryonic or neonatal lethality. We are currently investigating the mechanism of lethality. Surviving HO-1$^{-/-}$ mice were grossly normal and were used for subsequent experiments.

Chronic hypoxia increases right ventricular systolic pressure and ventricular weight in wild-type and HO-1$^{-/-}$ mice. To investigate the role of HO-1 in the response to hypoxia, we housed mice (five to six mice in each group) in a 10% oxygen environment for five to seven weeks. As expected, seven weeks of hypoxia caused hematocrit values to increase from 44.0 ± 1.4% to 73.0 ± 8.2% in wild-type mice. Similarly, hematocrit values increased from 40.0 ± 2.8% to 78.0 ± 5.9% in HO-1$^{-/-}$ mice. In contrast to rats (20, 30, 34), mice subjected to chronic hypoxia sustained rather modest pulmonary vascular remodeling (defined as an increase in peripheral muscularized vessels) (24, 35). Moreover, in our study, there was no significant difference in hypoxia-induced remodeling between wild-type and HO-1$^{-/-}$ mice at seven weeks (51% vs. 52.5% partially and completely muscularized peripheral vessels). We then determined the effect of hypoxia on right ventricular systolic pressure, which is an indicator of pulmonary arterial systolic pressure. Right ventricular systolic pressure in wild-type and HO-1$^{-/-}$ mice did not differ under normoxic conditions (P = 0.80; Figure 2a, open bars). Although five weeks of hypoxia increased right ventricular systolic pressure, it did so to a

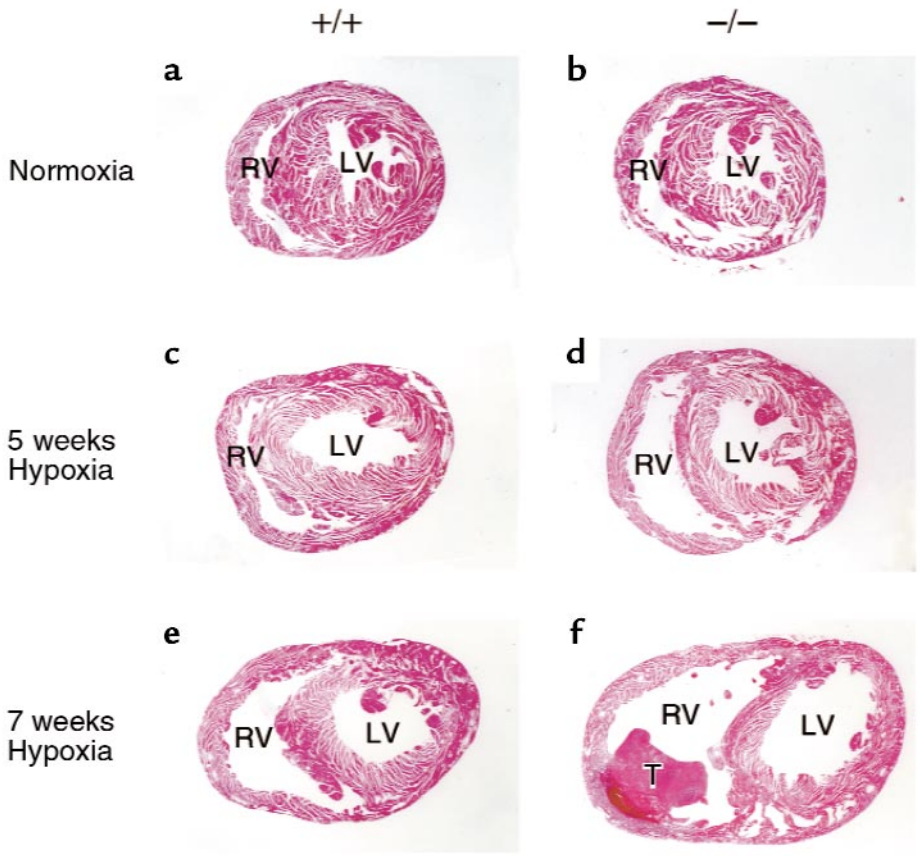

Figure 3
Right ventricular dilatation and thrombus formation in HO-1$^{-/-}$ mice in response to hypoxia. Heart cross-sections (at the papillary muscle level) from wild-type (+/+) and HO-1 null (–/–) mice were stained with hematoxylin and eosin (n = 5–6 in each group). Mice were exposed to normoxia (**a**, +/+; **b**, –/–), five weeks of hypoxia (**c**, +/+; **d**, –/–), or seven weeks of hypoxia (**e**, +/+; **f**, –/–). RV, right ventricle; LV, left ventricle; T, thrombus. Original magnification: ×15.

similar degree in wild-type and HO-1$^{-/-}$ mice (P = 0.43; Figure 2a, filled bars).

The ventricular weight index did not differ between wild-type and HO-1$^{-/-}$ mice under normoxic conditions (Figure 2b, open bars). Exposure to hypoxia for seven weeks caused a 32% increase in the ventricular weight index in wild-type mice. In HO-1$^{-/-}$ mice, however, the ventricular weight index after seven weeks of hypoxia increased 100% in comparison with that in normoxic wild-type mice (Figure 2b, filled bars). Studies in a subgroup of mice revealed that the changes in ventricular weight reflected mainly a right ventricular effect, as the RV/(LV + septum) increased in HO-1$^{-/-}$ mice in comparison with wild-type mice exposed to hypoxia for seven weeks (data not shown).

Hypoxia induces right ventricular infarcts and mural thrombi in HO-1$^{-/-}$ mice. Under normoxic conditions, there were no obvious histological differences between wild-type and HO-1$^{-/-}$ mice (Figure 3, a and b). After five weeks of hypoxia, HO-1$^{-/-}$ mice showed increased right ventricular dilatation (Figure 3d) in comparison with wild-type mice (Figure 3c). After seven weeks of hypoxia, the right ventricles in HO-1$^{-/-}$ mice were even more dilated (Figure 3f) than those in similarly treated wild-type mice (Figure 3e). Note that the right ventricular free wall from the HO-1$^{-/-}$ mouse (Figure 3f) does not appear thicker than the one from the wild-type mouse (Figure 3e). Remarkably, a large organized thrombus, attached to the infarcted right ventricular wall, is visible in the HO-1$^{-/-}$ mouse (Figure 3f). Four of six HO-1$^{-/-}$ hearts exposed to seven weeks of hypoxia showed evidence of right ventricular infarcts, and mural thrombi were present in all four infarcted right ventricles. Sections from one animal in each group (n = 5–6) are shown in Figure 3 because the histological analyses were similar under normoxic and hypoxic conditions within a particular group.

Chronic hypoxia induces right ventricular infarction in HO-1$^{-/-}$ mice. To search for additional evidence of infarcts in the right ventricle, we examined the tissue sections at higher magnifications. Cardiomyocytes were intact in ventricular sections from wild-type mice exposed to seven weeks of hypoxia (Figure 4, a and c). In contrast, ventricular sections from HO-1$^{-/-}$ mice exposed to seven weeks of hypoxia (Figure 4, b and d) showed mononuclear inflammatory cell infiltration and extensive cardiomyocyte degeneration and death with focal calcification (indicated by an arrow in Figure 4d); these characteristics are consistent with infarcts one to two weeks old. Moreover, the right ventricular infarcts did not appear to result from vascular occlusion, because the coronary arteries supplying blood to the right ventricle were patent in HO-1$^{-/-}$ mice (data not shown). To detect collagen accumulation indicative of fibrosis, we stained ventricular sections with Masson's trichrome. After seven weeks of hypoxia, cells surrounding blood vessels stained positive for collagen in hearts from wild-type mice (Figure 4e). In hearts from HO-1$^{-/-}$ mice exposed to seven weeks of hypoxia, however, early collagen deposition was present throughout the lesion (Figure 4f, beneath the thrombus). This degree of fibrosis is consistent with early scar formation and a lesion one to two weeks old.

Two of the six hearts examined in the HO-1$^{-/-}$ mice exposed to seven weeks of hypoxia did not exhibit gross right ventricular infarcts; however, close examination of these hearts revealed focal areas of myocardial degeneration without evidence of extensive inflammatory cell infiltration. These hearts showed early evidence of myocardial damage. Hearts from wild-type and HO-1$^{-/-}$ mice examined after five weeks of exposure

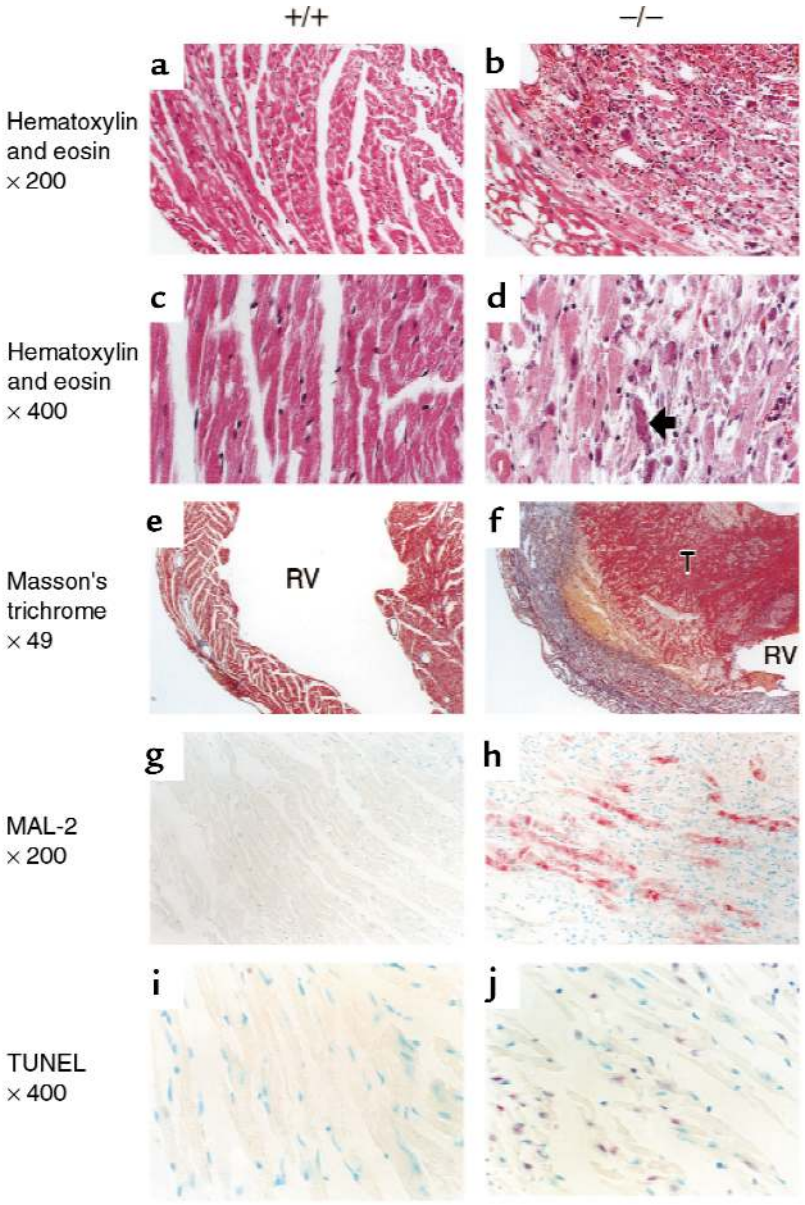

Figure 4
Histological analysis of wild-type and HO-1$^{-/-}$ mouse hearts after seven weeks of hypoxia. Six animals were examined in each group. Hematoxylin and eosin–stained right ventricular free wall from wild-type (+/+) mouse (**a** and **c**) and infarcted area of right ventricle (underneath thrombus) from HO-1 null (–/–) mouse (**b** and **d**). Original magnifications: ×200 (**a** and **b**) and ×400 (**c** and **d**). The dense areas of blue nuclei in **b** and **d**, not visible in **a** and **c**, represent mononuclear cell infiltrate. Wild-type (**e**) and HO-1$^{-/-}$ (**f**) heart sections were stained with Masson's trichrome to reveal collagen (blue). RV, right ventricle; T, thrombus. Original magnification: ×49. MAL-2–immunostained (pink) right ventricular free wall from wild-type mouse (**g**) and area of infarcted right ventricle (underneath thrombus) from HO-1$^{-/-}$ mouse (**h**). Original magnification: ×200. TUNEL assay for apoptotic cardiomyocytes in right ventricular free wall from wild-type mouse (**i**) and free wall (surrounding infarcted region) from HO-1$^{-/-}$ mouse (**j**). TUNEL-positive cardiomyocytes stained red. Original magnification: ×400.

to hypoxia displayed no cardiomyocyte degeneration or death and no extensive mononuclear inflammatory cell infiltration (data not shown). Cells surrounding blood vessels stained positive for collagen in hearts from wild-type and HO-1$^{-/-}$ mice housed for five weeks under normoxic and hypoxic conditions (data not shown). However, in contrast with the right ventricular free walls from HO-1$^{-/-}$ mice exposed to seven weeks of hypoxia, which showed deposition of collagen, no collagen deposition was evident in the right ventricular free walls from HO-1$^{-/-}$ mice exposed to five weeks of hypoxia. Taken together, these data confirm that in the HO-1$^{-/-}$ mice exposed to seven weeks of hypoxia, myocardial infarcts were less than two weeks old.

To assess oxidative damage in HO-1$^{-/-}$ hearts with infarcts, we immunostained ventricular sections with polyclonal antibody MAL-2, which recognizes oxidation-specific lipid-protein adducts. In contrast to the minimal MAL-2 staining in hearts from wild-type mice (Figure 4g), MAL-2 staining was intense in cells (predominantly cardiomyocytes) beneath the infarcted area of the right ventricle in HO-1$^{-/-}$ mice (Figure 4h). This difference suggests the presence of severe oxidative damage within and around the infarct site. We also performed TUNEL assays to detect the presence of DNA fragmentation and apoptosis in the hearts of HO-1$^{-/-}$ mice exposed to hypoxia. No TUNEL-positive cardiomyocytes were detected in right ventricles from wild-type mice (Figure 4i). In right ventricles from HO-1$^{-/-}$ mice, however, a significant number of TUNEL-positive cells surrounded the infarct site (Figure 4j).

Discussion

We show by gene-deletion experiments in vivo that HO-1 plays an important, protective role in the adaptation of the cardiovascular system to hypoxia. Right ventricles from HO-1$^{-/-}$ mice exposed to chronic hypoxia were severely dilated and contained right ventricular infarcts with mural thrombi (Figures 3 and 4).

The three characteristic responses of humans and animals to hypoxia are pulmonary vascular remodeling, pulmonary hypertension, and hypertrophy of the right ventricle (20–24). Hypoxia induces HO-1 expression in the lung (36), and CO generated by hypoxic VSMCs inhibits proliferation of these cells in culture (13, 25, 37). These links have suggested an important role for HO-1 in the regulation of hypoxia-induced pulmonary vascular remodeling. Our results indicate that chronic hypoxia–induced pulmonary vascular remodeling and pulmonary hypertension were similar in HO-1$^{-/-}$ and wild-type mice (Figure 2). Thus, the loss of HO-1 appears to have had little effect on these two responses after prolonged hypoxia. Perhaps CO released by HO-2 is sufficient to inhibit excessive pul-

monary vascular remodeling and hypertension in response to hypoxia. Alternatively, multiple vasoactive agents released within the pulmonary vasculature in the setting of chronic hypoxia may compensate for the lack of HO-1–derived CO.

As it does in rats (26), hypoxia increases HO-1 protein abundance (by approximately threefold in hearts of wild-type mice after seven weeks; data not shown). Our data show that the absence of HO-1 results in a maladaptive response in cardiomyocytes exposed to hypoxia-induced pulmonary hypertension. Although the myocardium in HO-1$^{-/-}$ mice appears to be normal under normoxic conditions, under hypoxic conditions, severe right ventricular dilatation and infarcts with mural thrombi develop in HO-1$^{-/-}$, but not wild-type, mice — despite exposure to similar hypoxia and pulmonary hypertension. These results are supported by reports indicating that HO-1 is induced in the heart after exposure to hypoxia and increased pulmonary arterial pressure and that HO-1 may have a protective effect on cardiomyocytes subjected to stress (1, 16, 17, 26). Mural thrombi can be detected in 28–40% of patients with acute myocardial infarction (38, 39). We observed mural thrombi in every mouse that had a right ventricular infarct. This high percentage of mural thrombi may be related to a combination of marked dilatation of the right ventricle and high hematocrit and blood viscosity values (even though the hematocrit value was similar in wild-type and HO-1$^{-/-}$ mice exposed to hypoxia). The absence of HO-1 may also increase platelet aggregation and predispose to thrombus formation, because CO has been shown to inhibit platelet aggregation (19, 40).

Our results demonstrate that cardiomyocytes in HO-1$^{-/-}$ mice die in response to hypoxia/pulmonary hypertension. Although some cardiomyocyte death appears to be due to necrosis, we did detect TUNEL-positive cells in the zone around the infarct (Figure 4j), which suggests apoptosis as one of the mechanisms leading to cardiomyocyte death. Hypoxia and elevated pulmonary arterial pressure increase cardiac production of reactive oxygen species (41, 42), which play a significant role in myocardial cell death during ischemia/reperfusion (43, 44). Also, overexpression of HO-1 protects against damage caused by oxidative stress in several cell types in vitro (45, 46). Thus, it is likely that the absence of HO-1 in cardiomyocytes leads to an accumulation of reactive oxygen species that causes cardiomyocyte death. This conclusion is supported by our finding of extensive lipid peroxidation in the zone of right ventricular infarction (Figure 4h) and by the findings of Poss and Tonegawa (47), who showed that HO-1$^{-/-}$ embryonic fibroblasts are more sensitive to cytotoxicity caused by hydrogen peroxide. Although myocardial infarction has been shown to increase oxidative stress (48, 49), we have found a two- to threefold increase in the nitration of protein tyrosine residues, which indicates the presence of the potent oxidant peroxynitrite, in noninfarcted HO-1$^{-/-}$ hearts exposed to seven weeks of hypoxia (data not shown). Thus, an increase in oxidative stress may precede gross myocardial infarction.

In summary, our results show that HO-1 is essential for cardiomyocytes to adapt to stresses such as hypoxia and subsequent pulmonary hypertension. The protective effect of HO-1 may be related to its antioxidant activity. The absence of coronary occlusion in HO-1$^{-/-}$ mice in combination with myocardial infarction and severe ventricular dilatation limited to the right side of the heart suggests a maladaptive response of cardiomyocytes to increased pulmonary arterial pressure. On the basis of these findings, we postulate that HO-1 may play a central role in cardiac physiology by protecting cardiomyocytes from pressure-induced injury and secondary oxidative damage. Our findings may lead to novel approaches for preventing cardiomyocyte damage due to hemodynamic stress or ischemia/reperfusion.

Acknowledgments

We are grateful to R. Rosenberg (Massachusetts Institute of Technology, Cambridge, Massachusetts, USA) for providing us with D3 ES cells, and H. Rayburn (Massachusetts Institute of Technology) for advice on ES cell culture. We thank T. Minamino (The Children's Hospital) for his assistance with the hypoxic chamber setup, and J. Witztum for providing the MAL-2 antibody. We also thank S. Folta, P. Marria, D. Zhang, D. Tenenholz, A. Patel, C. Sim, and B. Ith for technical assistance, and T. McVarish for editorial assistance.

This work was supported in part by an American Heart Association Grant-in-Aid (to M.A. Perrella); National Institutes of Health grants HL-60788 (to M.A. Perella), HL-53249 (to M.-E. Lee), HL-10113 (to M.D. Layne), and HL-55454 and HL-56398 (to S. Kourembanas); a grant from Novartis and the SICPA Foundation (to P. Wiesel); and a grant from the CHRC New Project Development Fund of the National Institute of Child Health and Human Development (to H. Christou).

1. Maines, M.D. 1997. The heme oxygenase system: a regulator of second messenger gases. *Annu. Rev. Pharmacol. Toxicol.* **37**:517–554.
2. Maines, M.D. 1988. Heme oxygenase: function, multiplicity, regulatory mechanisms, and clinical applications. *FASEB J.* **2**:2557–2568.
3. Pfeifer, A., *et al.* 1998. Defective smooth muscle regulation in cGMP kinase I-deficient mice. *EMBO J.* **17**:3045–3051.
4. Murad, F. 1994. Cyclic GMP: synthesis, metabolism, and function. Introduction and some historical comments. *Adv. Pharmacol.* **26**:1–5.
5. Stocker, R., et al. 1987. Bilirubin is an antioxidant of possible physiological importance. *Science.* **235**:1043–1046.
6. Stocker, R., Glazer, A.N., and Ames, B.N. 1987. Antioxidant activity of albumin-bound bilirubin. *Proc. Natl. Acad. Sci. USA.* **84**:5918–5922.
7. Shibahara, S., Muller, R., Taguchi, H., and Yoshida, T. 1985. Cloning and expression of cDNA for rat heme oxygenase. *Proc. Natl. Acad. Sci. USA.* **82**:7865–7869.
8. Maines, M.D., and Kappas, A. 1974. Cobalt induction of hepatic heme oxygenase; with evidence that cytochrome P-450 is not essential for this enzyme activity. *Proc. Natl. Acad. Sci. USA.* **71**:4293–4297.
9. Choi, A.M.K., and Alam, J. 1996. Heme oxygenase-1: function, regulation, and implication of a novel stress-inducible protein in oxidant-induced lung injury. *Am. J. Respir. Cell Mol. Biol.* **15**:9–19.
10. Trakshel, G.M., Kutty, R.K., and Maines, M.D. 1986. Purification and characterization of the major constitutive form of testicular heme oxygenase. The noninducible isoform. *J. Biol. Chem.* **261**:11131–11137.
11. Trakshel, G.M., and Maines, M.D. 1989. Multiplicity of heme oxygenase isozymes. HO-1 and HO-2 are different molecular species in rat and rabbit. *J. Biol. Chem.* **264**:1323–1328.
12. McCoubrey, W.K., Jr., Huang, T.J., and Maines, M.D. 1997. Isolation and characterization of a cDNA from the rat brain that encodes hemoprotein heme oxygenase-3. *Eur. J. Biochem.* **247**:725–732.
13. Morita, T., Perrella, M.A., Lee, M.E., and Kourembanas, S. 1995. Smooth muscle cell-derived carbon monoxide is a regulator of vascular cGMP. *Proc. Natl. Acad. Sci. USA.* **92**:1475–1479.
14. Borger, D.R., and Essig, D.A. 1998. Induction of HSP 32 gene in hypoxic cardiomyocytes is attenuated by treatment with *N*-acetyl-L-cysteine. *Am. J. Physiol.* **274**:H965–H973.
15. Yet, S.-F., *et al.* 1997. Induction of heme oxygenase-1 expression in vascular smooth muscle cells. A link to endotoxic shock. *J. Biol. Chem.* **272**:4295–4301.
16. Sharma, H.S., Maulik, N., Gho, B.C., Das, D.K., and Verdouw, P.D. 1996. Coordinated expression of heme oxygenase-1 and ubiquitin in the porcine heart subjected to ischemia and reperfusion. *Mol. Cell. Biochem.* **157**:111–116.
17. Pellacani, A., *et al.* 1998. Induction of heme oxygenase-1 during endotoxemia is downregulated by transforming growth factor-β1. *Circ. Res.* **83**:396–403.
18. Camhi, S.L., *et al.* 1995. Induction of heme oxyge-

nase-1 gene expression by lipopolysaccharide is mediated by AP-1 activation. *Am. J. Respir. Cell Mol. Biol.* **13**:387–398.
19. Wagner, C.T., *et al.* 1997. Hemodynamic forces induce the expression of heme oxygenase in cultured vascular smooth muscle cells. *J. Clin. Invest.* **100**:589–596.
20. Tucker, A., *et al.* 1975. Lung vascular smooth muscle as a determinant of pulmonary hypertension at high altitude. *Am. J. Physiol.* **228**:762–767.
21. Herget, J., Suggett, A.J., Leach, E., and Barer, G.R. 1978. Resolution of pulmonary hypertension and other features induced by chronic hypoxia in rats during complete and intermittent normoxia. *Thorax*. **33**:468–473.
22. Meyrick, B., and Reid, L. 1980. Ultrastructural findings in lung biopsy material from children with congenital heart defects. *Am. J. Pathol.* **101**:527–542.
23. Hales, C.A., Kradin, R.L., Brandstetter, R.D., and Zhu, Y.J. 1983. Impairment of hypoxic pulmonary artery remodeling by heparin in mice. *Am. Rev. Respir. Dis.* **128**:747–751.
24. Klinger, J.R., *et al.* 1993. Cardiopulmonary responses to chronic hypoxia in transgenic mice that overexpress ANP. *J. Appl. Physiol.* **75**:198–205.
25. Morita, T., *et al.* 1997. Carbon monoxide controls the proliferation of hypoxic vascular smooth muscle cells. *J. Biol. Chem.* **272**:32804–32809.
26. Katayose, D., Isoyama, S., Fujita, H., and Shibahara, S. 1993. Separate regulation of heme oxygenase and heat shock protein 70 mRNA expression in the rat heart by hemodynamic stress. *Biochem. Biophys. Res. Commun.* **191**:587–594.
27. Alam, J., Cai, J., and Smith, A. 1994. Isolation and characterization of the mouse heme oxygenase-1 gene. Distal 5′ sequences are required for induction by heme or heavy metals. *J. Biol. Chem.* **269**:1001–1009.
28. Healy, A.M., *et al.* 1995. Absence of the blood-clotting regulator thrombomodulin causes embryonic lethality in mice before development of a functional cardiovascular system. *Proc. Natl. Acad. Sci. USA*. **92**:850–854.
29. Laird, P.W., *et al.* 1991. Simplified mammalian DNA isolation procedure. *Nucleic Acids Res.* **19**:4293.
30. Christou, H., *et al.* 1998. Increased vascular endothelial growth factor production in the lungs of rats with hypoxia-induced pulmonary hypertension. *Am. J. Respir. Cell Mol. Biol.* **18**:768–776.
31. Rosenfeld, M.E., *et al.* 1990. Distribution of oxidation specific lipid-protein adducts and apolipoprotein B in atherosclerotic lesions of varying severity from WHHL rabbits. *Arteriosclerosis*. **10**:336–349.
32. Gavrieli, Y., Sherman, Y., and Ben-Sasson, S.A. 1992. Identification of programmed cell death in situ via specific labeling of nuclear DNA fragmentation. *J. Cell Biol.* **119**:493–501.
33. Poss, K.D., and Tonegawa, S. 1997. Heme oxygenase 1 is required for mammalian iron reutilization. *Proc. Natl. Acad. Sci. USA*. **94**:10919–10924.
34. Underwood, D.C., *et al.* 1998. Chronic hypoxia-induced cardiopulmonary changes in three rat strains: inhibition by the endothelin receptor antagonist SB 217242. *J. Cardiovasc. Pharmacol.* **31**:S453–S455.
35. Steudel, W., *et al.* 1998. Sustained pulmonary hypertension and right ventricular hypertrophy after chronic hypoxia in mice with congenital deficiency of nitric oxide synthase 3. *J. Clin. Invest.* **101**:2468–2477.
36. Lee, P.J., *et al.* 1997. Hypoxia-inducible factor-1 mediates transcriptional activation of the heme oxygenase-1 gene in response to hypoxia. *J. Biol. Chem.* **272**:5375–5381.
37. Morita, T., and Kourembanas, S. 1995. Endothelial cell expression of vasoconstrictors and growth factors is regulated by smooth muscle cell–derived carbon monoxide. *J. Clin. Invest.* **96**:2676–2682.
38. Lamas, G.A., Vaughan, D.E., and Pfeffer, M.A. 1988. Left ventricular thrombus formation after first anterior wall acute myocardial infarction. *Am. J. Cardiol.* **62**:31–35.
39. Vecchio, C., *et al.* 1991. Left ventricular thrombus in anterior acute myocardial infarction after thrombolysis. A GISSI-2 connected study. *Circulation*. **84**:512–519.
40. Brune, B., and Ullrich, V. 1987. Inhibition of platelet aggregation by carbon monoxide is mediated by activation of guanylate cyclase. *Mol. Pharmacol.* **32**:497–504.
41. Kehrer, J.P., and Park, Y. 1991. Oxidative stress during hypoxia in isolated-perfused rat heart. *Adv. Exp. Med. Biol.* **283**:299–304.
42. Park, Y., and Kehrer, J.P. 1991. Oxidative changes in hypoxic-reoxygenated rabbit heart: a consequence of hypoxia rather than reoxygenation. *Free Radic. Res. Commun.* **14**:179–185.
43. Vanden Hoek, T.L., *et al.* 1998. Reactive oxygen species released from mitochondria during brief hypoxia induce preconditioning in cardiomyocytes. *J. Biol. Chem.* **273**:18092–18098.
44. Baines, C.P., Goto, M., and Downey, J.M. 1997. Oxygen radicals released during ischemic preconditioning contribute to cardioprotection in the rabbit myocardium. *J. Mol. Cell. Cardiol.* **29**:207–216.
45. Lee, P.J., Alam, J., Wiegand, G.W., and Choi, A.M. 1996. Overexpression of heme oxygenase-1 in human pulmonary epithelial cells results in cell growth arrest and increased resistance to hyperoxia. *Proc. Natl. Acad. Sci. USA*. **93**:10393–10398.
46. Motterlini, R., *et al.* 1996. NO-mediated activation of heme oxygenase: endogenous cytoprotection against oxidative stress to endothelium. *Am. J. Physiol.* **270**:H107–H114.
47. Poss, K.D., and Tonegawa, S. 1997. Reduced stress defense in heme oxygenase 1-deficient cells. *Proc. Natl. Acad. Sci. USA*. **94**:10925–10930.
48. Hill, M.F., and Singal, P.K. 1996. Antioxidant and oxidative stress changes during heart failure subsequent to myocardial infarction in rats. *Am. J. Pathol.* **148**:291–300.
49. Hill, M.F., and Singal, P.K. 1997. Right and left myocardial antioxidant responses during heart failure subsequent to myocardial infarction. *Circulation*. **96**:2414–2420.